ACS OMEGA

Open Access

http://pubs.acs.org/journal/acsodf

Article

Characterization of Potential Plastic-Degradation Enzymes from Marine Bacteria

Jin Jin and Zongchao Jia*

Cite This: *ACS Omega* 2024, 9, 32185−32192

Read Online

ACCESS | Metrics & More | Article Recommendations | Supporting Information

ABSTRACT: Polyethylene terephthalate (PET) and polyethylene (PE) are prominent polymer materials that comprise a significant portion of commercial plastic waste. Their durability and slow degradation rate have resulted in significant accumulation of plastic on Earth. In a recent study, macrotranscriptomic profiling of a reconstituted marine bacterial community identified 10 putative enzymes capable of directly acting on PE or PET (PEases or PETases). Among these enzymes, three recombinant proteins were reported to possess PE degradation activity. To select potential plastic degrading enzyme candidates for protein engineering efforts, we expressed and purified eight out of the 10 candidates, excluding two due to poor expression and/or solubility. Notably, several candidate proteins displayed significant esterase activity on *p*-nitrophenyl butyrate and exhibited unexpected thermostability despite their marine origin. Additionally, we observed dose- and time-dependent hydrolytic activity on the PET trimer substrate. Structural analysis and mutagenesis of a candidate protein confirmed the presence of catalytic triad residues, classifying it as an esterase. Furthermore, we elucidated the structural importance of the two disulfide bonds. Through point mutation experiments, we observed an enhanced hydrolytic activity of a selected enzyme candidate on PET nanoparticles. Our findings challenge the classification of the enzymes directly acting on PE and highlight the significance and complexity of validating PE degradation enzymes identified through metagenomic analysis.

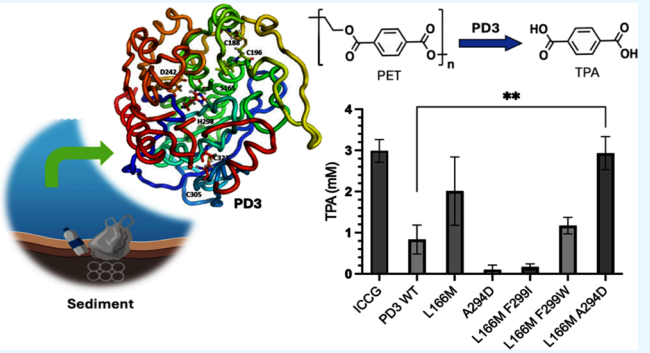

INTRODUCTION

Polyethylene terephthalate (PET) and polyethylene (PE) constitute a significant portion of commercial plastic waste, comprising 10.2 and 36.3% of the plastic market, respectively.[1] Their tenacity and extremely low degradation rate have resulted in the rapid accumulation of plastic waste on Earth, exerting a profound impact on our environment.[2] Enzymatic degradation of PET and PE offers an environmentally friendly alternative compared to conventional disposal methods, such as landfills and incineration, which often lead to inadvertent environmental release.

PET is a heteroatomic polymer composed of terephthalic acid (TPA) and ethylene glycol (EG) linked by ester bonds. Due to its relatively facile degradability, there has been active research into the enzymatic degradation of PET. PET degrading enzymes (PETases) primarily belong to the esterases (EC3.1.1), catalyzing the hydrolysis of ester bonds to depolymerize PET to EG, TPA, mono(2-hydroxyethyl) terephthalic acid (MHET), or bis(2-hydroxyethyl) terephthalic acid (BHET). Numerous PETases have been found across various biospheres, including bacteria and fungi. Particularly noteworthy is *Is*PETase, a putative lipase isolated from *Ideonella sakaiensis* 201-F6, which exhibited an impressive PET degrading activity.[3] The development of *Is*PETase combined with advanced evolution engineering techniques such as rational engineering and machine learning has led to significant improvements in PET enzymatic degradability, yielding enzymes like Dura-PETase[4] and FAST-PETase.[5] Cutinases, such as *Tf*Cut2 from *Thermobifida fusca* and leaf-branch compost cutinase (LCC), have been extensively investigated for their PET hydrolytic activities.[6,7] Variants resulting from evolutionary engineering studies of LCC, including ICCG (F243I/D238C/S283C/Y127G) and WCCG (F243W/D238C/S283C/Y127G), have demonstrated enhanced stability compared to the wild type.[8]

In contrast to PET, PE is a high-molecular-weight hydrophobic compound consisting solely of inert C−C and C−H bonds. The initial step in PE biodegradation, likely involving the oxidation of inactive C−H bonds, is expected to be the limiting factor due to the high stability of these bonds. The discovery of enzymes that can directly act on PE (PEases) poses a significant challenge, largely attributed to the unclear

Received: May 22, 2024
Revised: June 29, 2024
Accepted: July 5, 2024
Published: July 8, 2024

Table 1. Potential Plastic Degrading Enzymes

	Genbank ID	locus_tag	source	function
PD1	QPI65985.1	IR195_09930	*Halomonas venusta*	hydrolase
PD2	QPI64981.1	IR195_04495	*Halomonas venusta*	α/β fold hydrolase
PD3	QPA27412.1	IR196_16650	*Brucella anthropi*	α/β fold hydrolase
PD4	QPI67555.1	IR194_14175	*Exiguobacterium* sp.	LysM peptidoglycan-binding domain-containing protein
PD5	QPI66471.1	IR194_08235	*Exiguobacterium* sp.	G-D-S-L family lipolytic protein
PD6	QPI67435.1	IR194_13555	*Exiguobacterium* sp.	α/β fold hydrolase
PD7	QPI68731.1	IR194_05420	*Exiguobacterium* sp.	α/β fold hydrolase
PD8	QPI68425.1	IR194_03795	*Exiguobacterium* sp.	α/β hydrolase
PD9	QPI66066.1	IR195_10375	*Halomonas venusta*	response regulator transcription factor
PD10	QPA26456.1	IR196_00850	*Brucella anthropi*	α/β fold hydrolase

mechanism of PE enzymatic degradation.[9] Certain secreted enzymes such as manganese peroxidases (MnP), lignin peroxidases (LiP), and laccases have been implicated in the oxidation of waste PE in the environment.[10−12] Notably, two enzymes from the waxworm *Galleria mellonella* have been recombinantly expressed and verified to possess PE oxidization capabilities.[13] However, individually purified or recombinantly expressed direct PE-acting enzymes typically exhibited only limited PE degradation activity.[9] As a result, research on PEases still remains in the discovery stage, predominantly focusing on finding *bona fide* direct PE-acting enzymes.

Metagenomic studies have proven to be a highly valuable tool for the identification of PETases or PEases, offering promising prospects for sustainable plastic recycling, upcycling, and mitigating plastic pollution. Employing such an approach, Gao and Sun recently reported 10 putative PET or PE degrading enzymes in a reconstituted bacterial community sourced from a marine consortium CAS6, which exhibited promising degradation activities on both PE and PET films.[14] These potential plastic enzymes were identified through macrotranscriptomic profiling of a reconstituted marine bacterial community that exhibited a degrading effect on both PET and PE. Somewhat surprisingly, the direct PE degradability of three recombinant enzymes was shown by preliminary degradation assays.

In the current study, we sought to recombinantly express all 10 candidates identified in Gao's research (Table 1), renamed them as PD proteins (plastic degrading proteins), and characterize their potential activities and stability. Among these PD proteins, PD1, PD2, and PD3 were claimed to have PE degrading activities by Gao et al.[14] Using a variety of substrates, we determined the plastic degrading activity of selected candidates. The catalytic triad and two disulfate bonds of PD3 were probed by site-directed mutagenesis. PD3, PD5, and PD8 showed modest PET nanoparticle (PET NP) degradability. PD3 variants demonstrated increased hydrolytic activity compared to the wild type.

MATERIALS AND METHODS

Stains, Plasmids, and Mutagenesis. The candidate enzymes in this work are listed in Table 1. Plasmid cloning and mutagenesis were conducted in *Escherichia coli* (*E. coli*) DH5a. The genes encoding PD1, PD2, and PD3 were cloned into the pET21b vector using restriction enzymes NdeI and XhoI. 6His-MBP-tag-fused PD4−PD10 were cloned into a customized pET28a vector via *Bam*HI and XhoI. To enhance protein expression and purification, the PD2 gene was transferred into a customized pET21b-based vector, HT29 (6His-MBP-TEV-protein), while the PD3 gene was moved into a customized pET21b-based vector, HT2 (protein-6His), to increase the yield and purity. The positive PETase control, LCC, and an engineered variant of LCC, ICCG, were cloned into HT2 via *Bam*HI and XhoI. Insertion and deletion mutagenesis was executed via PCR as described.[15] Oligonucleotide primers used are given in Table S1. Constructs and mutations were verified by whole-plasmid sequencing (Plasmidsaurus) or Sanger sequencing (TCAG facilities).

Bacterial Protein Expression and Purification. Recombinant protein expression was conducted using *E. coli* BL21(DE3) RIPL. Bacteria were cultured in LB broth and supplemented with either ampicillin or kanamycin depending on the specific plasmid used. Overnight cultures were inoculated at 1/100 dilution into a fresh Terrific broth (TB) medium supplemented with a selective antibiotic at 37 °C in a shaker at 180 rpm until the optical density (OD_{600}) reached 0.6, at which point expression was induced with 0.2 mM IPTG. Subsequently, cultures were allowed to grow overnight at 16 °C. Cells were harvested by centrifugation and resuspended in a lysis buffer composed of 50 mM Tris pH 8.0, 500 mM NaCl, 10% glycerol, and 3 mM 2-mercaptoethanol. Cells were lysed via sonication with a Branson instrument for 7 min, with cycles of 5 s on and 15 s off. Lysates were clarified via centrifugation at 18,000 rpm for 30 min. The clarified supernatant was subjected to the appropriate resin (amylose for MBP-tagged proteins, NEB E8021L; Ni-NTA for His-tagged proteins, Cytiva 17057502). After washing with a lysis buffer, proteins were eluted with either 10 mM maltose or 200 mM imidazole depending on the tag used. Further purification of PD proteins was performed by size exclusion chromatography in a buffer (pH 8.0) composed of 20 mM Tris and 150 mM NaCl. Cells overexpressing LCC and ICCG were pelleted and resuspended in a lysis buffer containing 50 mM Tris pH 7.0, 500 mM NaCl, 10% glycerol, and 3 mM 2-mercaptoethanol. Purification of LCC and ICCG was carried out using Ni-NTA chromatography in the lysis buffer, and size exclusion chromatography was conducted in a buffer (pH 7.0) composed of 20 mM Tris and 150 mM NaCl, as they served as positive PETases in the assays.

Esterase Activity Assay. The esterase activity of PD proteins was determined on a 96-well plate as previously described.[16] Briefly, the reaction was performed in a 100 mM potassium phosphate buffer (pH 7.4) containing 25 μM PD proteins and 0.5 mM substrate *p*-nitrophenyl butyrate (p-NPB, C = 4) and incubated at 37 °C for 30 min. The production of *p*-nitrophenol (ε_{400} = 0.0148 M^{-1} cm^{-1}) was monitored at 400 nm using a microtiter plate reader (SpectraMax iD3, Molecular Devices, LLC). One unit of enzyme activity was defined as the release of 1.0 nM *p*-nitrophenol per minute at pH 7.4 and 37

https://doi.org/10.1021/acsomega.4c04843
ACS Omega 2024, 9, 32185−32192

°C. For PD3, other substrates, such as *p*-nitrophenyl hexanoate (p-NPH, $C = 6$) and *p*-nitrophenyl octanoate (p-NPO, $C = 8$), were also assayed, and pH and temperature were optimized. The Michaelis−Menten plot of PD3 was obtained using different concentrations of the substrate, p-NPB. V_{max} and K_m were analyzed using Prism 10 software.

Determination of Protein Stability. PD protein stability was determined in a buffer (pH 8.0) composed of 20 mM Tris and 150 mM NaCl. A protein thermal shift was measured using an SYPRO orange protein gel stain (Invitrogen) and a CFX Opus 96 real-time PCR system (Bio-Rad, US).[17] In brief, 45 μL of a protein at a concentration of 5 μM was mixed with 5 μL of a 200× SYPRO orange dye before subjecting it to a temperature-rising protocol ranging from 25 to 100 °C with 0.5 °C steps for 30 s.

Circular dichroism (CD) spectroscopy was used to examine the response of the protein's secondary structure to increasing temperatures.[18] Approximately 300 μL of a 1 mg/mL protein stock was dispensed into a round cuvette, and the sample was heated incrementally in 2.5 °C steps. After each temperature was reached, the ellipticity of the sample was recorded across the wavelength range of 180−260 nm. To determine the melting temperature (T_m) value, the fraction unfolded (F_U) was calculated using the formula $F_U = (F_O - F)/(U_F - F)$, where F_O represents the ellipticity value at the lowest peak for each temperature, F is the average value of F_O when the protein is unfolded, and U_F is the average value of the F_O where protein is unfolded. The graph was plotted with F_U against temperature and fit into the Boltzmann equation. The T_m value is equal to the temperature at which F_U equals 0.5.

3PET Hydrolysis Activity Assay. A model substrate for PETase, 3PET, was employed to assess the hydrolytic activity of PET oligomers of PD proteins. The conversion of 3PET to the water-soluble TPA, benzoic acid, and EG results in a decrease in the turbidity of emulsified 3PET, serving as a measure of enzymatic activity. Emulsified 3PET solution was prepared as described previously.[19] Briefly, 50 mg of 3PET was dissolved in 1.5 mL of acetone with 20 mg of the surfactant, Plysurf A210G. The mixture was then slowly added to 20 mL of 50 mM Tris at pH 8.0 with vigorously stirring. Afterward, sonication was performed for 15 min by using a pulse of 3 s on and 4 s off. Acetone removal was achieved by stirring the mixture in the fume hood at 50 °C for 2 h and then by overnight stirring at room temperature.

For the agar plate assay, 5 μL of the purified enzyme was added to a small well created on 3PET agar plates containing a 1.5% 3PET emulsion in agarose. The plate was then incubated at 30 °C for 20 h, and the hydrolytic activity was assessed by observing the cleared halo around the well. In the 3PET turbidity assay conducted in a 96-well plate, the emulsified 3PET solution was diluted with 50 mM Tris at pH 8.0 to achieve an OD of approximately 1 at 580 nm. Subsequently, 40 μL of the enzyme was added to 160 μL of the diluted 3PET emulsion, and the turbidity at 580 nm was monitored to determine the hydrolytic activity. LCC was included as a positive control.

PET Nanoparticle Hydrolytic Activity. PET NP were prepared as previously described by Pfaff et al.[20] In brief, PET NP were dissolved in 1,1,1,3,3,3-hexafluoro-2-propanol (HFIP) and then resuspended in water followed by sonication. HFIP was then removed by vacuum evaporation. The hydrolytic reaction system consisted of 10 μL of PET NP solution, 40 μL of the reaction buffer (100 mM Na_3PO_4, pH 8.0), 50 μL of distilled water, and 100 μL of enzyme solution. The reaction was conducted at 30 °C for 4 days. A 100 mM NaOH solution was used to fully deprotonate TPA and produce terephthalate initially. Additionally, the use of hydroxyl radicals to generate 2-hydroxyterephthalate, which exhibits stable fluorescence, provides a sensitive and efficient method for detecting TPA. TPA production was measured by hydroxylating 150 μL of the reaction system supernatant with 25 μL of 5 mM EDTA and 25 μL of 5 mM Fe(II)SO_4 in a black 96-well plate for fluorometric readings. Fluorescence emission at 421 nm upon excitation at 315 nm was recorded using a microtiter plate reader (SpectraMax iD3, Molecular Devices, LLC). A standard curve was established using 2-hydroxyterephthalate generated from the TPA concentration ranging from 0.0625 to 5 mM. The TPA content in the hydrolysis product of each enzyme was quantified using the established standard curve and normalized to mM per mg of the enzyme.

RESULTS

Esterase Activity of PD Proteins. To optimize protein expression, we experimented with different fusion tags (His- or MBP-tag) and locations (N- or C-terminus). For example, in the case of PD2, the expression yield and purity were optimal upon fusion with an MBP-tag at the N-terminus. Similarly, the expression of PD3 was substantially improved when the His-tag was relocated from the N-terminus to the C-terminus (Figure S1). Eight candidates were successfully expressed and purified, except for PD4 and PD10, which exhibited poor expression and/or solubility. PD1 was expressed with an N-terminal His-tag. PD3 was expressed with a C-terminal His-tag, while the remaining constructs (PD2, PD5−PD9) were expressed with an N-terminal His-MBP-tag. SDS-PAGE analysis of PD protein purification is shown in Figure S2.

Subsequently, we assessed the esterase activity of the eight recombinant PD proteins using the substrate *p*-nitrophenyl butyrate (p-NPB). Among these candidates, PD3, PD5, and PD8 displayed relatively high esterase activity, whereas PD2 and PD6 exhibited only slight activity. PD1, PD7, and PD9 demonstrated relatively low or undetectable levels of esterase activity under the tested conditions (Figure 1).

Stability of PD3, PD5, and PD8. Due to the high crystallinity of postconsumer PET plastics, industrial plastic

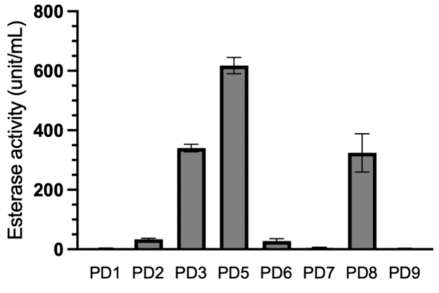

Figure 1. Esterase activity of recombinant PD enzymes. The assay was performed in a 100 mM potassium phosphate buffer at pH 7.4 and 37 °C for 30 min with a 25 μM enzyme and a 0.5 mM p-NPB substrate. The production of 4-nitrophenol was monitored at 400 nm in a microtiter plate reader. One unit of esterase is defined as the amount of the enzyme needed to release 1 nM *p*-nitrophenol per minute at pH 7.4 and 37 °C. The data represent $n = 3$ technical replicates, with error bars showing ± standard deviation.

https://doi.org/10.1021/acsomega.4c04843
ACS Omega 2024, 9, 32185−32192

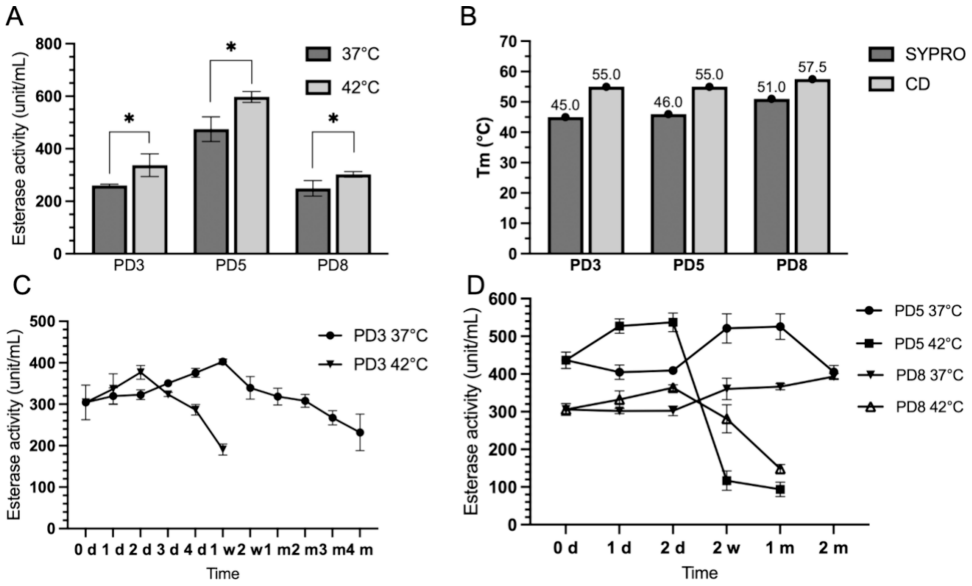

Figure 2. Stability of PD3, PD5, and PD8. (A) Esterase activity of PD3, PD5, and PD8 measured at 37 and 42 °C using p-NPB. (B) Stability determined from the melting temperature for PD3, PD5, and PD8 using SYPRO and CD analysis. (C) Long-term stability of PD3. (D) Long-term stability of PD5 and PD8. The data represent $n = 3$ technical replicates. Two-way ANOVA; ns, $p > 0.05$, *$p < 0.1$, **$p < 0.01$. Error bars represent ± standard deviation.

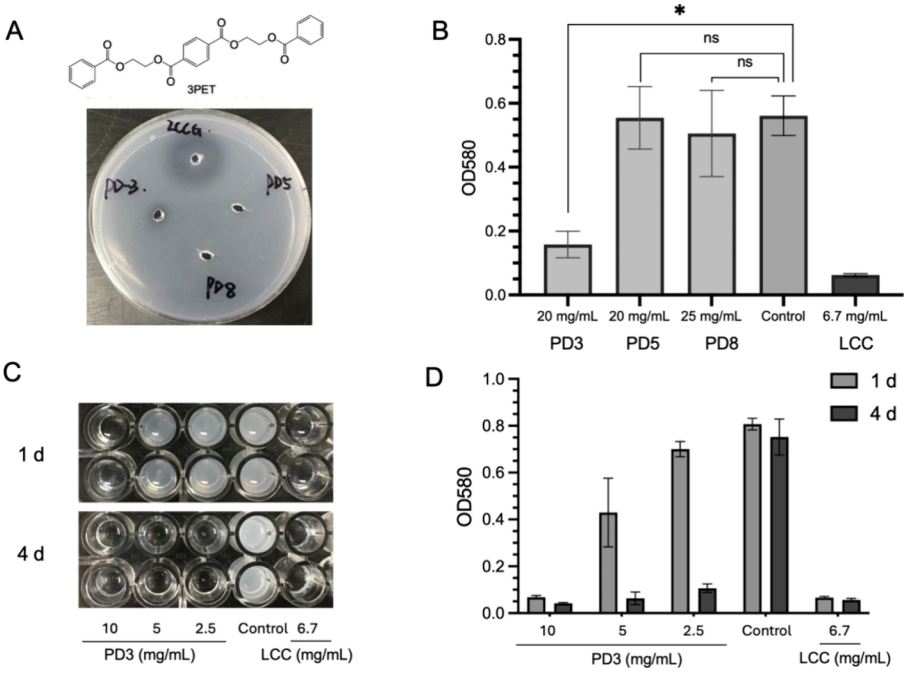

Figure 3. 3PET hydrolytic activity of PD proteins. (A) Structure of 3PET and 3PET hydrolytic activity of PD proteins observed as the hydrolysis zone on an agarose plate containing 3PET after 20 h of incubation with PD candidates at 30 °C. (B) Turbidity of the 3PET emulsified solution after 20 h of incubation with PD candidates at 30 °C. (C,D) Turbidity of the 3PET emulsified solution after 1 and 4 days of incubation with different concentrations of PD3 at 30 °C or buffer (control). LCC was used as a positive control. The data represent $n = 2$ technical replicates. Two-way ANOVA; ns, $p > 0.05$, *$p < 0.1$, **$p < 0.01$. Error bars represent ± standard deviation.

degradation is typically performed at temperatures above its glass transition temperature (>70 °C). Therefore, we evaluated the stability of the PD enzymes exhibiting good esterase activity. PD3, PD5, and PD8 demonstrated enhanced esterase activity at 42 °C compared to 37 °C (Figure 2A). The protein thermal shift assay conducted using an SYPRO orange dye and the CFX Opus 96 real-time PCR system revealed that PD3, PD5, and PD8 could be denatured at temperatures of 45, 46, and 51 °C, respectively. Circular dichroism (CD) analysis determined the melting temperatures of these three candidates to be 55, 55, and 57.5 °C, respectively (Figure 2B).

We further monitored the long-term stability of PD3, PD5, and PD8 by storing them at 37 or 42 °C and periodically checked their activities at 37 °C. Interestingly, PD3 exhibited increased esterase activity during the first week at 37 °C, which then returned to its original level after one month, retaining 79.0% activity after 4 months of incubation at 37 °C. Conversely, when stored at 42 °C for 1 week, PD3's activity

https://doi.org/10.1021/acsomega.4c04843
ACS Omega 2024, 9, 32185−32192

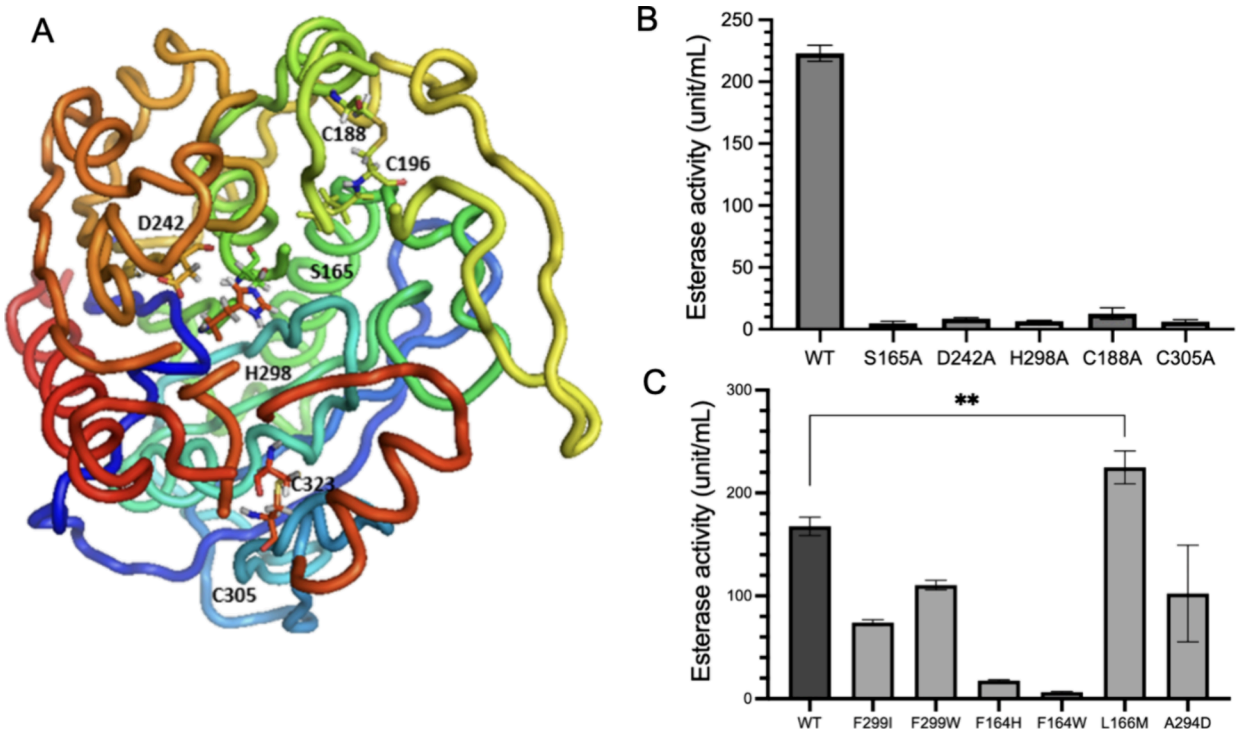

Figure 4. (A) Predicted structural model of PD3. (B) Comparison of esterase activity between inactivation mutations and wildtype PD3. (C) Comparison of esterase activity between the mutants and wildtype PD3. The data represent $n = 3$ technical replicates. Two-way ANOVA; ns, $p > 0.05$, $*p < 0.1$, $**p < 0.01$. Error bars represent ± standard deviation.

significantly decreased, retaining only 56.4% activity (Figure 2C). PD5 and PD8 maintained their activity at 37 °C for at least two months, whereas protein denaturation and decreased activity were observed after 2 weeks at 42 °C (Figure 2D).

Since PD3 possesses the best long-term stability, further characterization of PD3's esterase activity was performed using different ester substrates with varying lengths of the carbon chain, such as *p*-nitrophenyl hexanoate (p-NPH, $C = 6$) and *p*-nitrophenyl octanoate (p-NPO, $C = 8$). The Michaelis–Menten plot indicated that the V_{max} was 394.4 nM/min/mg and K_m was 7.824 mM (Figure S3A). Higher activities of PD3 were observed when using p-NPB and p-NPH at 42 °C compared with 37 °C (Figure S3B). The optimal activity was at pH 7.5 (Figure S3C). When the esterase assay was performed at temperatures above 37 °C, such as 42, 50, and 55 °C, the activity of PD3 stored at 37 °C increased with increasing temperature (Figure S3D). However, at temperatures of 50 °C or higher, PD3 was degraded after 30 min.

3PET Hydrolytic Activity of PD Candidates. Bis-(benzoyloxyethyl) terephthalate (3PET), which is essentially a short chain of PET and thus represents a more relevant substrate than p-NPB, was utilized as a substrate for a measurement of PET hydrolytic activity. 3PET emulsions were introduced into the agar, and clear hydrolysis zones were observed surrounding the sample holes upon 3PET degradation. ICCG was employed as a positive control in this assay. Among the tested candidates, PD3 at a concentration of 1 mg/mL exhibited slight 3PET hydrolytic activity after 20 h of incubation at 30 °C (Figure 3A). No zones of clearance in the agar were observed around PD5 and PD8, indicating their lack of activity.

Next, a turbidity assay was conducted by adding a 3PET emulsion into a 96-well plate; PD3 exhibited significant hydrolytic activity after 20 h of incubation at 30 °C. PD3 concentrations ranging from 2.5 to 10 mg/mL were added to the 3PET emulsion, and the assay was conducted for 1 and 4 days at 30 °C. Subsequent analysis revealed that the 3PET hydrolytic activity of PD3 was both dose-dependent and time-dependent (Figure 3C).

Our findings suggest that PD3 possesses favorable properties for PET degradation, including esterase activity, stability, and 3PET hydrolytic activity. Consequently, we selected PD3 as a template for further analysis and engineering. However, the discovery that PD3 is an esterase eliminates the possibility of it being a direct PE-acting enzyme, as PE lacks ester bonds, unlike PET.

The Catalytic Triad of PD3. To analyze the key residues of PD3 for engineering design, a predicted structure of PD3 was obtained using Phyre2 (Figure 4A).[21] The classical conserved catalytic triad of hydrolases comprises a serine, an aspartic acid, and a histidine.[22] Protein stabilization via disulfide bonds is a common feature in thermophilic organisms and has been successfully implemented in strategies to enhance the stability of proteins.[23] PETases with excellent degradation activity typically possess one or two disulfide bonds. Notably, *Is*PETase harbors two disulfide bonds (Cys239-Cys203 and Cys273-Cys289) in its active sites, contributing to its stability.[24] *Tf*Cut2 contains one disulfide bond believed to be responsible for the additional stability.[25] Based on the amino acid sequence and the predicted structure of PD3 (Figure 4A), we postulated that S165, D242, and H298 constitute the catalytic triad due to the relative positioning of the residues. Two disulfide bonds were anticipated, one between C188 and C196 and the other between C305 and C323. Subsequently, S165A, D242A, and H298A mutants of PD3 were generated to verify the catalytic triad. As expected, all three mutations completely abolished the PD3's activity.

https://doi.org/10.1021/acsomega.4c04843
ACS Omega 2024, 9, 32185−32192

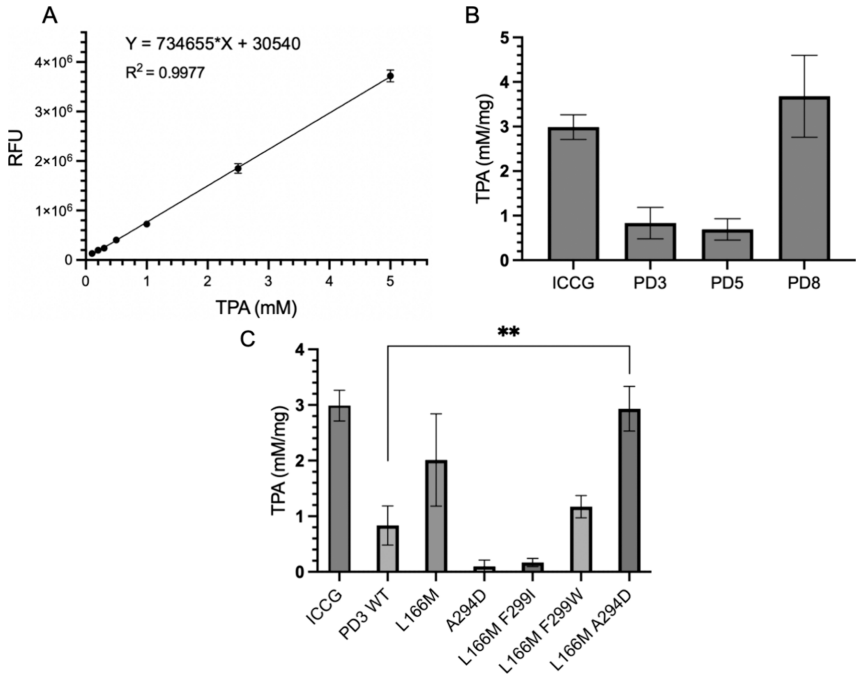

Figure 5. PET NP hydrolytic activity of PD proteins. (A) Standard curve created using a gradient concentration of TPA. (B) TPA released from PET NP was normalized to mM per mg of the enzyme after treatment with PD proteins at a concentration of 10 mg/mL, and positive control ICCG was quantified using a standard curve. (C) TPA products of PET NP was normalized to mM per mg of the enzyme after treatment with PD3 variants and wildtype PD3 at a concentration of 10 mg/mL. ICCG was used as a positive control. A hydrolytic reaction system was composed of 10 μL of PET NP solution, 40 μL of a reaction buffer (100 mM Na_3PO_4, pH 8.0), 50 μL of distilled water, and 100 μL of enzyme solution. The reaction was carried out at 30 °C for 4 days. TPA production was detected by hydroxylating 150 μL of the supernatant of the reaction system with 25 μL of 5 mM EDTA and 25 μL of 5 mM Fe(II)SO_4. Fluorescence emission at 421 nm upon excitation at 315 nm was obtained using a microtiter plate reader. A standard curve was established using 0.0625 to 5 mM TPA incubated with 25 μL of 5 mM EDTA and 25 μL of 5 mM Fe(II)SO_4. The data represent n = 3 technical replicates. Two-way ANOVA; ns, $p > 0.05$, *$p < 0.1$, **$p < 0.01$. Error bars represent ± standard deviation.

Moreover, replacing C188 or C305 with alanine significantly affected PD3's activity (Figure 4B).

Mutations of PD3 aimed at improving esterase activity were designed based on conserved residues found in classical PETases (Table S2). The GXSXG motif, highly conserved among several published PETases, including *Is*PETase and LCC—two PETases that have undergone significant improvement through evolutional engineering[8,24]—guided our design process. Single mutant variants PD3 F164H and PD3 F164W were designed by replacing the first X in the GXSXG motif within PD3 with the corresponding residues in the catalytic triad of LCC and *Is*PETase. PD3 L166M was obtained by replacing the second X in the motif within PD3 with the residue following the serine in the catalytic triad of *Is*PETase. Additionally, F299I and F299W mutations were designed based on a report of increased PET depolymerization in LCC.[8] The DG/NATHF motif, containing a histidine in the catalytic triad, is conserved across type 1 PETases, such as LCC, Cut190, and *Tf*Cut2.[26] This motif exists in the primary sequence of PD3 as AGATHF. We obtained variant PD3 A294D by replacing residue A294 with aspartic acid. Subsequently, esterase assays were conducted on these single mutation variants using a supernatant of the expression culture lysates, and L166M demonstrated increased esterase activity by 34% compared to the wildtype PD3 (Figure 4C).

PET Nanoparticle Hydrolytic Activity of PD3. We next utilized PET nanoparticles (PET NP) as a substrate to assess whether PD proteins can hydrolyze long-chain polymers. The production of TPA from PET NP serves as an indicator of the PET degradation activity. Initially, a standard curve of TPA was established using a range of concentrations from 0.0625 to 5 mM (Figure 5A). PD3, PD5, and PD8 demonstrated PET NP hydrolytic activity at high concentrations, despite PD5 and PD8 not exhibiting 3PET hydrolytic activity (Figure 5B). The PD3 variant L166M exhibited enhanced TPA production compared to wildtype PD3, suggesting an improvement in PET hydrolysis activity. To further improve PD3's activity, double mutant variants containing L166M, such as PD3 L166M/F299I, L166M/F299W, and L166M/A294D, were created. L166M/F299W and L166M/A294D exhibited enhanced TPA production compared to wildtype PD3 (Figure 5C).

■ DISCUSSION

The intriguing observation that both the marine consortium CAS6 and the reconstituted bacterial community exhibit proficiency in degrading PE and PET is noteworthy,[14] although the PE degrading activity is somewhat surprising. This discovery warrants further investigation of individual enzymes in the pursuit of enzyme catalysts capable of facilitating plastic recycling. Through transcriptomic profiling of the reconstituted bacterial community, 10 proteins were identified as potential plastic degrading enzymes.[14] Among these, PD4-PD8 exhibited conspicuous increases in gene expression when the bacterial community was supplemented with PET, in comparison to the control lacking PET. Meanwhile, the gene expressions of the remaining five enzymes, PD1−3, PD9, and PD10, were upregulated when the culture was supplemented with PE. A validation study was conducted on 3 putative direct PE-acting enzymes, PD1, PD2,

https://doi.org/10.1021/acsomega.4c04843
ACS Omega 2024, 9, 32185−32192

and PD3, employing recombinant proteins. Based on SEM data, these enzymes were claimed to degrade PE films. For example, PD3 induced visible morphological changes in PE films at a concentration of 0.1 mg/mL after 24 h at 30 °C.

To characterize all 10 putative candidates, recombinant proteins were expressed in *E. coli*. Except for PD4 and PD10, recombinant proteins for the other candidates were obtained with high yields and purities by fusing an MBP-tag at the N-terminus of the protein. For PD3, expression was optimized by fusing a 6xHis-tag at the C-terminus instead of the N-terminus. Based on their classification, all candidates were categorized as hydrolases. Specifically, PD9 was identified as a cutinase, while PD1, PD4, and PD5 were classified as a hydrolase and PD2, PD3, PD6, PD7, PD8, and PD10 as α/β hydrolases (Table 1). Esterase (EC3.1.1) represents a primary subclass of hydrolase that catalyzes the hydrolysis of ester bonds. In this study, PD2, PD3, PD5, PD6, and PD8 were identified as esterases using p-NPB as a substrate. Notably, PD3, PD5, and PD8 exhibited significant esterase activity at 37 °C. Furthermore, stability is another substantial property for plastic degrading enzymes, quantified as the T_m. T_m values of PD3, PD5, and PD8, as detected by CD, were ∼5 °C higher than the data obtained by the orange dye method. Assessing long-term stabilities investigated by incubation at a certain temperature and activity monitoring provides more reliable data. PD3 outstood minimal activity loss after 2 months, retaining 79% esterase activity following 4 months of incubation at 37 °C, suggesting an attractive target for further exploration.

Within the α/β hydrolase family, ∼75% contains a Ser-His-Asp catalytic triad. The catalytic triad of PD3 was proposed based on its predicted structure and the primary sequence, subsequently confirmed through single-site mutagenesis. Furthermore, the cysteines responsible for forming disulfide bonds were found to be essential for esterase activity. The GXSXG motif, highly conserved among various types of PETases,[24] is present within PD3. When the second "X" in the GXSXG motif of PD3, L166, was mutated to methionine, the residue highly conserved following the serine in the catalytic triad of PETases, enhanced esterase activity, and hydrolytic activity of PET NP were observed compared to the wildtype PD3. This suggests that this residue plays an important role in ester bond hydrolysis. The DGATHF motif, containing histidine in the catalytic triad, was found to be conserved across type 1 PETases, such as Cut190 and *Tf*Cut2,[26] which also exists in PD3 as AGADHF. Replacing the A294 of PD3 variant L166 M to aspartic acid resulted in a significant improvement in hydrolysis activity compared to the wildtype PD3, indicating that both residues are essential for PET hydrolysis.

Upregulated gene expression of hydrolases has been observed in several omics studies apart from Gao and Sun's research.[14] For example, the PE degrading effect of three marine bacterial isolates was attributed to the production of three bacterial esterases.[27] In a mechanism study of PE degradation, it was revealed that esterases participate in hydrolysis after oxidized PE was converted to an ester by Baeyer−Villiger monooxygenases (BVMO).[28] Upregulated expression of lipase, esterase, and cutinase was detected during the PE degradation process, with esters detected in the products of PE degradation, suggesting the potential involvement of these hydrolases in PE degradation. However, the precise mechanism by which these hydrolases participate in the PE degrading process remains unknown. Further exploration is required to understand the PE degradabilities of these enzymes.

In addition to PETases or putative direct PE-acting enzymes within the marine consortium network, the enzymes upregulated in the presence of PET or PE may likely involve other factors for plastic degradation. For example, they may require another reaction partner to effectively act on the plastics such as a redox partner, as is commonly required by monooxygenases. PET can undergo depolymerization through hydrolysis, whereas PE presents a far more recalcitrant molecule. The absence of functional groups in PE hampers hydrolysis and other common transformations since its biodegradation would necessitate the introduction of functional groups, often achieved through oxidation.[9]

Since the sequences of the PD enzymes clearly suggest a function akin to lipase, esterase, cutinase, or hydrolase and a lack of homology with known oxidase or oxygenase enzymes, which typically catalyze the first modification step in PE prior to chain breakage,[9] it is unlikely that these hydrolases upregulated in the presence of PE possess putative activity toward PE. PE does not contain ester bonds, and its breakdown requires oxidation as a prior step before the yet-unclear chain cleavage reaction.[9]

The considerably different performance noted between the reconstituted bacterial community and individual enzymes could stem from either selecting enzymes that do not directly participate in plastic breakdown or the necessity of a combination of proteins, possibly from the same or different species, to degrade the plastics effectively. Moreover, in addition to genes encoding plastic degrading enzymes, genes related to biofilm formation, bacterial secretion, and cell growth/reproduction would also undergo significant upregulation in a plastic-rich environment. Taken together, these studies underscore the formidable challenge of identifying *bona fide* protein candidates capable of degrading PE directly.[9] They further highlight the importance of scrutinizing the activity of putative enzymes that can directly act on PE.

■ ASSOCIATED CONTENT

Supporting Information

The Supporting Information is available free of charge at https://pubs.acs.org/doi/10.1021/acsomega.4c04843.

(Figure S1) Purification of PD2 and PD3 recombinant proteins, (Figure S2) purification of PD proteins using Ni-NTA or amylose resin, (Figure S3) characterization of esterase activity of PD3, (Table S1) primers in this study, and (Table S2) protein sequence and catalytic triad of PD3 and other known PETases (PDF)

Accession Codes

Accession Codes: PD1, QPI65985.1; PD2, QPI64981.1; PD3, QPA27412.1; PD4, QPI67555.1; PD5, QPI66471.1; PD6, QPI67435.1; PD7, QPI68731.1; PD8, QPI68425.1; PD9, QPI66066.1; PD10, QPA26456.1.

■ AUTHOR INFORMATION

Corresponding Author

Zongchao Jia − *Department of Biomedical and Molecular Sciences, Queen's University, Kingston, ON KL7 3N6, Canada;* orcid.org/0000-0002-9322-9394; Phone: 613 533-6277; Email: jia@queensu.ca

https://doi.org/10.1021/acsomega.4c04843
ACS Omega 2024, 9, 32185−32192

Author

Jin Jin − *Department of Biomedical and Molecular Sciences, Queen's University, Kingston, ON KL7 3N6, Canada*

Complete contact information is available at: https://pubs.acs.org/10.1021/acsomega.4c04843

Notes

The authors declare no competing financial interest.

■ ACKNOWLEDGMENTS

We would like to acknowledge the assistance provided by Dr. Graeme Howe and Dr. David Zechel from Queen's University, Dr. Karine Auclair and Jane Arciszewski from McGill University, and Dr. Sofia Lemak from the University of Toronto. This work was funded by the Government of Canada through Genome Canada and Ontario Genomics (OGI-207).

■ REFERENCES

(1) Inderthal, H.; Tai, S. L.; Harrison, S. T. L. Non-Hydrolyzable Plastics - An Interdisciplinary Look at Plastic Bio-Oxidation. *Trends Biotechnol* **2021**, *39* (1), 12−23.

(2) Chamas, A.; Moon, H.; Zheng, J.; Qiu, Y.; Tabassum, T.; Jang, J. H.; Abu-Omar, M.; Scott, S. L.; Suh, S. Degradation Rates of Plastics in the Environment. *ACS Sustainable Chem. Eng.* **2020**, *8* (9), 3494−3511.

(3) Yoshida, S.; Hiraga, K.; Takehana, T.; Taniguchi, I.; Yamaji, H.; Maeda, Y.; Toyohara, K.; Miyamoto, K.; Kimura, Y.; Oda, K. A bacterium that degrades and assimilates poly(ethylene terephthalate). *Science* **2016**, *351* (6278), 1196−1199.

(4) Cui, Y.; Chen, Y.; Liu, X.; Dong, S.; Tian, Y. e.; Qiao, Y.; Mitra, R.; Han, J.; Li, C.; Han, X.; et al. Computational Redesign of a PETase for Plastic Biodegradation under Ambient Condition by the GRAPE Strategy. *ACS Catal.* **2021**, *11* (3), 1340−1350.

(5) Lu, H.; Diaz, D. J.; Czarnecki, N. J.; Zhu, C.; Kim, W.; Shroff, R.; Acosta, D. J.; Alexander, B. R.; Cole, H. O.; Zhang, Y.; et al. Machine learning-aided engineering of hydrolases for PET depolymerization. *Nature* **2022**, *604* (7907), 662−667.

(6) Wei, R.; Breite, D.; Song, C.; Gräsing, D.; Ploss, T.; Hille, P.; Schwerdtfeger, R.; Matysik, J.; Schulze, A.; Zimmermann, W. Biocatalytic Degradation Efficiency of Postconsumer Polyethylene Terephthalate Packaging Determined by Their Polymer Microstructures. *Advanced Science* **2019**, *6* (14), 1900491.

(7) Sulaiman, S.; Yamato, S.; Kanaya, E.; Kim, J. J.; Koga, Y.; Takano, K.; Kanaya, S. Isolation of a novel cutinase homolog with polyethylene terephthalate-degrading activity from leaf-branch compost by using a metagenomic approach. *Appl. Environ. Microbiol.* **2012**, *78* (5), 1556−1562.

(8) Tournier, V.; Topham, C. M.; Gilles, A.; David, B.; Folgoas, C.; Moya-Leclair, E.; Kamionka, E.; Desrousseaux, M. L.; Texier, H.; Gavalda, S.; et al. An engineered PET depolymerase to break down and recycle plastic bottles. *Nature* **2020**, *580* (7802), 216−219.

(9) Jin, J.; Arciszewski, J.; Auclair, K.; Jia, Z. Enzymatic polyethylene biorecycling: Confronting challenges and shaping the future. *Journal of Hazardous Materials* **2023**, *460*, No. 132449.

(10) Iiyoshi, Y.; Tsutsumi, Y.; Nishida, T. Polyethylene degradation by lignin-degrading fungi and manganese peroxidase. *Journal of Wood Science* **1998**, *44* (3), 222−229.

(11) Ehara, K.; Iiyoshi, Y.; Tsutsumi, Y.; Nishida, T. Polyethylene degradation by manganese peroxidase in the absence of hydrogen peroxide. *Journal of Wood Science* **2000**, *46* (2), 180−183.

(12) Zhang, A.; Hou, Y.; Wang, Q.; Wang, Y. Characteristics and polyethylene biodegradation function of a novel cold-adapted bacterial laccase from Antarctic sea ice psychrophile Psychrobacter sp. NJ228. *J. Hazard Mater.* **2022**, *439*, No. 129656.

(13) Sanluis-Verdes, A.; Colomer-Vidal, P.; Rodriguez-Ventura, F.; Bello-Villarino, M.; Spinola-Amilibia, M.; Ruiz-Lopez, E.; Illanes-Vicioso, R.; Castroviejo, P.; Aiese Cigliano, R.; Montoya, M.; et al. Wax worm saliva and the enzymes therein are the key to polyethylene degradation by Galleria mellonella. *Nat. Commun.* **2022**, *13* (1), 5568.

(14) Gao, R.; Sun, C. A marine bacterial community capable of degrading poly(ethylene terephthalate) and polyethylene. *Journal of Hazardous Materials* **2021**, *416*, No. 125928.

(15) Watson, J. F.; García-Nafría, J. In vivo DNA assembly using common laboratory bacteria: A re-emerging tool to simplify molecular cloning. *J. Biol. Chem.* **2019**, *294* (42), 15271−15281.

(16) Nolasco-Soria, H.; Moyano-López, F.; Vega-Villasante, F.; del Monte-Martínez, A.; Espinosa-Chaurand, D.; Gisbert, E.; Nolasco-Alzaga, H. Lipase and phospholipase activity methods for marine organisms. *Lipases and Phospholipases: Methods and Protocols* **2018**, *1835*, 139−167.

(17) Huynh, K.; Partch, C. L. Analysis of protein stability and ligand interactions by thermal shift assay. *Curr. Protoc. Protein Sci.* **2015**, *79*, 28.9.1−28.9.14.

(18) Greenfield, N. J. Using circular dichroism spectra to estimate protein secondary structure. *Nat. Protoc* **2006**, *1* (6), 2876−2890.

(19) Ribitsch, D.; Heumann, S.; Trotscha, E.; Herrero Acero, E.; Greimel, K.; Leber, R.; Birner-Gruenberger, R.; Deller, S.; Eiteljoerg, I.; Remler, P.; et al. Hydrolysis of polyethyleneterephthalate by p-nitrobenzylesterase from Bacillus subtilis. *Biotechnol. Prog.* **2011**, *27* (4), 951−960.

(20) Pfaff, L.; Breite, D.; Badenhorst, C. P. S.; Bornscheuer, U. T.; Wei, R. Chapter Twelve - Fluorimetric high-throughput screening method for polyester hydrolase activity using polyethylene terephthalate nanoparticles. In *Methods Enzymol.*, Weber, G.; Bornscheuer, U. T.; Wei, R., Eds.; Vol. *648*; Academic Press, 2021; pp 253−270.

(21) Kelley, L. A.; Mezulis, S.; Yates, C. M.; Wass, M. N.; Sternberg, M. J. The Phyre2 web portal for protein modeling, prediction and analysis. *Nat. Protoc* **2015**, *10* (6), 845−858.

(22) Rauwerdink, A.; Kazlauskas, R. J. How the Same Core Catalytic Machinery Catalyzes 17 Different Reactions: the Serine-Histidine-Aspartate Catalytic Triad of α/β-Hydrolase Fold Enzymes. *ACS Catal.* **2015**, *5* (10), 6153−6176.

(23) Zhu, B.; Wang, D.; Wei, N. Enzyme discovery and engineering for sustainable plastic recycling. *Trends Biotechnol.* **2022**, *40* (1), 22−37.

(24) Joo, S.; Cho, I. J.; Seo, H.; Son, H. F.; Sagong, H.-Y.; Shin, T. J.; Choi, S. Y.; Lee, S. Y.; Kim, K.-J. Structural insight into molecular mechanism of poly(ethylene terephthalate) degradation. *Nat. Commun.* **2018**, *9* (1), 382.

(25) Roth, C.; Wei, R.; Oeser, T.; Then, J.; Föllner, C.; Zimmermann, W.; Sträter, N. Structural and functional studies on a thermostable polyethylene terephthalate degrading hydrolase from Thermobifida fusca. *Appl. Microbiol. Biotechnol.* **2014**, *98* (18), 7815−7823.

(26) Bollinger, A.; Thies, S.; Knieps-Grünhagen, E.; Gertzen, C.; Kobus, S.; Höppner, A.; Ferrer, M.; Gohlke, H.; Smits, S. H. J.; Jaeger, K.-E. A Novel Polyester Hydrolase From the Marine Bacterium Pseudomonas aestusnigri − Structural and Functional Insights. *Front. Microbiol.* **2020**, *11*, 114.

(27) Khandare, S. D.; Agrawal, D.; Mehru, N.; Chaudhary, D. R. Marine bacterial based enzymatic degradation of low-density polyethylene (LDPE) plastic. *Journal of Environmental Chemical Engineering* **2022**, *10* (3), No. 107437.

(28) Zadjelovic, V.; Erni-Cassola, G.; Obrador-Viel, T.; Lester, D.; Eley, Y.; Gibson, M. I.; Dorador, C.; Golyshin, P. N.; Black, S.; Wellington, E. M. H.; et al. A mechanistic understanding of polyethylene biodegradation by the marine bacterium Alcanivorax. *Journal of Hazardous Materials* **2022**, *436*, No. 129278.